PROCEEDINGS OF SCIENCE

Measurement of Lepton Flavor Universality in B decays at Belle

S. Choudhury*
IIT Hyderabad
On behalf of Belle Collaboration
E-mail: ph16resch11007@iith.ac.in

We test the lepton flavor universality, $R_{K^{(*)}}$, in $B \to K^{(*)}\ell^+\ell^-$ ($\ell = e, \mu$) decays using a data sample of 711 fb^{-1} that contains 772×10^6 $B\bar{B}$ events. The data were collected at the $\Upsilon(4S)$ resonance with the Belle detector at the KEKB asymmetric-energy e^+e^- collider. The ratio R_{K^*} is measured in bins of dilepton invariant-mass squared, q^2; > 0.045, [0.1 - 8.0], [15.0 - 19.0], [0.045 - 1.1] and [1.1 - 6.0] GeV$^2/c^4$. Similarly, R_K is measured in q^2 bin of [0.1 - 4.0], [4.0 - 8.12], [1.0 - 6.0], > 14.18 and > 0.1 GeV$^2/c^4$. The results are found to be consistent with SM expectation.

We have also measured the $CP-$averaged isospin asymmetries (A_I) in different q^2 bins for $B \to K\ell^+\ell^-$ mode. The A_I has negative asymmetry for almost all the bins with the largest deviation of 2.7 standard deviations in $q^2 \in (1.0, 6.0)$ GeV$^2/c^4$ bin for $B \to K\mu^+\mu^-$ channel.

European Physical Society Conference on High Energy Physics - EPS-HEP2019 -
10-17 July, 2019
Ghent, Belgium

*Speaker.

PoS(EPS-HEP2019)259

1. Introduction

The decays $B \to K^{(*)}\ell^+\ell^-$ ($\ell = e, \mu$), which are propagated by the $b \to s$ quark-level transition, are flavor-changing neutral current processes. Such processes are forbidden at tree level in the standard model (SM) but can proceed via suppressed penguin or box diagrams, and are sensitive to particles predicted in a number of new physics models [1, 2]. Lepton-flavor-universality (LFU) ratio is a robust observable [3] to test the SM,

$$R_H = \frac{\int \frac{d\Gamma}{dq^2}[B \to H\mu^+\mu^-]dq^2}{\int \frac{d\Gamma}{dq^2}[B \to He^+e^-]dq^2}, \tag{1.1}$$

where H is a K or K^* meson and the decay rate Γ is integrated over a range of the dilepton invariant-mass squared, $q^2 = M^2(\ell^+\ell^-)$. For R_{K^*}, recently LHCb [4] reported hints of deviations from SM expectations at a level of $2.1-2.3$ standard deviation (σ) for low $q^2 \in (0.045, 1.1)\,\mathrm{GeV}^2/c^4$ and $2.4-2.5$ σ for central $q^2 \in (1.1, 6.0)$ bin. LHCb also measured R_K [5], reporting a difference of about 2.5 σ from the SM prediction in the $q^2 \in (1.1, 6.0)\,\mathrm{GeV}^2/c^4$ bin. Previous measurement of the same quantity was performed by Belle [6] in the whole q^2 range with a data sample of 657×10^6 $B\bar{B}$ events and result was consistent with SM prediction. The result presented here is obtained from a multi-dimensional fit, performed on the full Belle data sample, and supersedes our previous result.

Another theoretically robust observable [7], where the dominant form-factor-related uncertainties cancel, is the CP-averaged isospin asymmetry, that measures the difference in partial widths,

$$A_I = \frac{(\tau_{B^+}/\tau_{B^0})\mathscr{B}(B^0 \to K^0\ell^+\ell^-) - \mathscr{B}(B^+ \to K^+\ell^+\ell^-)}{(\tau_{B^+}/\tau_{B^0})\mathscr{B}(B^0 \to K^0\ell^+\ell^-) + \mathscr{B}(B^+ \to K^+\ell^+\ell^-)}, \tag{1.2}$$

where $\tau_{B^+}/\tau_{B^0} = 1.076$ is the lifetime ratio of B^+ to B^0 [8]. The A_I value is close to zero in the SM [9]. Earlier, BaBar [10], Belle [6] and LHCb [11] had reported A_I to be significantly below zero, especially in the q^2 region below the J/ψ resonance.

2. Belle Detector

The Belle detector is a large-solid-angle magnetic spectrometer composed of a silicon vertex detector (SVD), a 50-layer central drift chamber (CDC), an array of aerogel threshold Cherenkov counters (ACC), a barrel-like arrangement of time-of-flight scintillation counters (TOF), and an electromagnetic calorimeter (ECL) comprising CsI(Tl) crystals. All these are located inside a superconducting solenoid coil that provides a 1.5 T magnetic field. An iron flux return yoke placed outside the coil is instrumented with resistive plate chambers (KLM) to detect K_L^0 mesons and muons. Further details about the detector can be found in Ref. [12]. Two inner detector configurations were used: a 2.0 cm radius beam-pipe and a three-layer SVD for the first sample of $140\,\mathrm{fb}^{-1}$; and a 1.5 cm radius beam-pipe, a four-layer SVD, and a small-cell inner CDC for the remaining $571\,\mathrm{fb}^{-1}$ [13].

3. Test of LFU (R_{K^*}) in $B \to K^*\ell^+\ell^-$ decays

R_{K^*} is measured in Belle using a data sample of 711 fb^{-1} [14]. The decay modes reconstructed for this study are $B^0 \to K^{*0}\ell^+\ell^-$ and $B^+ \to K^{*+}\ell^+\ell^-$, where $\ell = e, \mu$. The K^* decays to $K^+\pi^-$, $K^+\pi^0$ and $K^0_S\pi^+$. The charge particles are selected which satisfies the PID criteria and near the interaction point. K^0_S candidates are reconstructed with an efficiency of 74% from pairs of oppositely charged tracks (treated as pions) by applying selection criteria on their invariant mass and vertex fit, π^0 are reconstructed from photon pairs, which satisties $E_\gamma > 30$ MeV and $115\ \mathrm{MeV/c^2} < \mathrm{M}_{\gamma\gamma} < 153\ \mathrm{MeV/c^2}$. The K^* candidate is combined with two oppositely charged leptons to form a B candidate.

The kinematic variables those distinguish signal from background are beam energy constraint mass, $M_{bc} = \sqrt{E^2_{beam}/c^4 - |p_B|^2/c^2}$, and the energy difference, $\Delta E = E_B - E_{beam}$, where E_B and p_B are the energy and momentum of B candidate, and E_{beam} is the beam energy. The candidate is selected when $5.22 < M_{bc} < 5.30$ GeV/c^2 and $-0.10\ (-0.05) < \Delta E < 0.05$ GeV for electron (muon) final states. The background contribution coming from J/ψ and $\psi(2S)$ are removed by applying $-0.25\ (-0.15) < M_{\ell\ell} - m_{J/\psi} < 0.08$ GeV$^2/c^4$ and $-0.20\ (-0.10) < M_{\ell\ell} < m_{\psi(2S)} < 0.08$ GeV$^2/c^4$ for the electron (muon) channel, respectively. A multivariate analysis technique, Neutral Network (NN), is developed to identify each particle type in the decay chain. The background coming from continuum ($q\bar{q} \to u\bar{u}, d\bar{d}, c\bar{c}, s\bar{s}$) and generic B ($q\bar{q} \to b\bar{b}$) are removed by applying optimal cut on top level NN, which is trained with some event shape and vertex quality variables. The signal is extracted by performed extended maximum likelihood fit to the M_{bc} distribution.

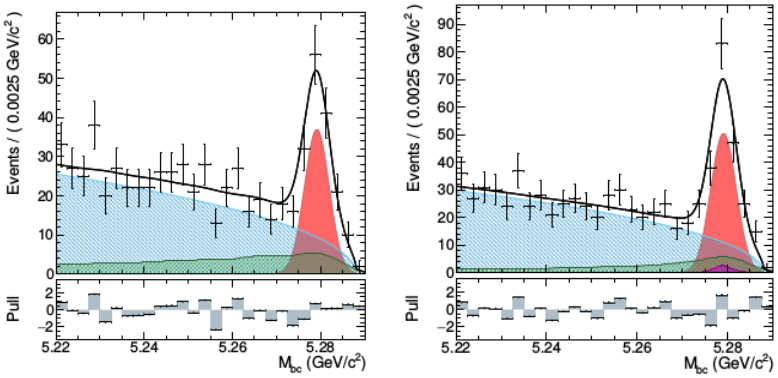

Figure 1: M_{bc} signal yield fit for the electron (left) and muon (right) modes with $q^2 > 0.045\,\mathrm{GeV}^2/c^4$. Combinatorial, signal, charmonium and peaking are shown as dashed blue, red filled, dashed green, purple dotted. The total component is shown as solid line superimposed on data points with error bars.

From the fit, there are $103.0^{+13.4}_{-12.7}$ ($139.9^{+16.0}_{-15.0}$) events in electron (muon) modes in the range $q^2 > 0.045$ GeV$^2/c^4$, respectively. The fit results are demonstrated in Figure 1. The R^*_K is calculated using Eqs. (1.1) for charged, neutral and combined cases. This is the first ever measurement of $R_{K^{*+}}$. All the measurements are found to be consistent with SM prediction and the results are shown in Figure 2.

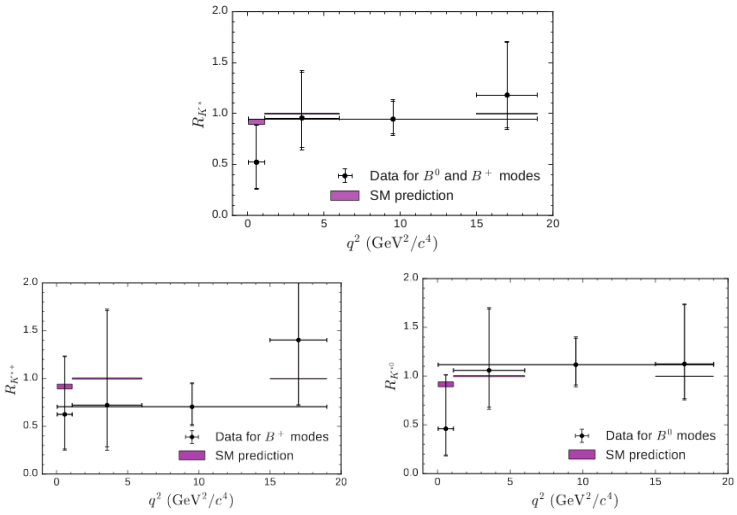

Figure 2: Results of R_{K^*} (upper), $R_{K^{*+}}$ (lower left) and $R_{K^{*0}}$ (lower right) compared to SM prediction. The separate vertical error bars indicate the statistical and total uncertainty.

4. Test of LFU (R_K) in $B \to K\ell\ell$ decays

The variable which can also verify the lepton flavor non universality is R_K in $B \to K\ell^+\ell^-$ decays. This R_K is calculated in Belle with a full data sample of 711 fb^{-1}[15]. The modes reconstructed for this study are $B^+ \to K^+\ell^+\ell^-$ and $B^0 \to K^0_S\ell^+\ell^-$, where $\ell = e, \mu$. The charged particles like $K^\pm$, $\mu^\pm$ and $e^\pm$ are selected which satisfies the PID criteria and near the interaction point. The K^0_S mesons are reconstructed by combining two oppositely charged tracks, assuming pion mass for both, with an invariant mass between 487 and 508 MeV, this corresponds to 3 σ window around the K^0_S nominal mass. The energy emitted by high energy electrons due to bremsstrahlung radiation are collected in a cone of 50 mrad around the initial momentum direction of the track.

To separate signal from background, the boundary on kinematic variables are $5.2 < M_{bc} < 5.29$ GeV/c^2 and $-0.1 < \Delta E < 0.25$ GeV. The decays $B \to J/\psi(\to \ell^+\ell^-)K$ and $B \to \psi(2S)(\to \ell^+\ell^-)K$, later used as control samples, are suppressed by applying a set of vetoes *i.e.*, $8.75 < q^2 < 10.2$ GeV$^2/c^4$ and $13.0 < q^2 < 14.0$ GeV$^2/c^4$ with the dimuon; $8.5 < q^2 < 10.2$ GeV$^2/c^4$ and $12.8 < q^2 < 14.0$ GeV$^2/c^4$ with the dielectron final states, respectively. To suppress the contamination from $\gamma^* \to e^+e^-$ and $\pi^0 \to \gamma e^+e^-$ a low q^2 (< 0.05) veto is applied. We have significant background from continuum and other B decays. To suppress these backgrounds we trained the NN with some event shape, kinematic and vertex quality variables. The NN output ($\mathscr{O}$) is translated to a new variable ($\mathscr{O}'$) using a log function,

$$\mathscr{O}' = \log\left(\frac{\mathscr{O} - \mathscr{O}_{\rm min}}{\mathscr{O}_{\rm max} - \mathscr{O}}\right) \tag{4.1}$$

where, $\mathscr{O}_{\rm min}$ and $\mathscr{O}_{\rm max}$ are the lower and upper boundaries of $\mathscr{O}$. The $\mathscr{O}_{\rm max}$ value depends on the decay mode and is determined from the signal MC. The $\mathscr{O}_{\rm min}$ applied is -0.6 and this reduces the background by $> 75\%$ with $4-5\%$ of signal efficiency loss. The peaking background which mimic signal, one is candidates arising from $B^+ \to \bar{D}^0(K^+\pi^-)\pi^+$ and is found in $B^+ \to K^+\mu^+\mu^-$

mode because of misidentification of pions as muons. The background is suppressed by applying $M_{K^+\mu^-} \notin (1.85-1.88)$ GeV/c^2. Another peaking is from $B^+ \to J/\psi(\to \mu^+\mu^-)K^+$ in which one of the muon is misidentified as kaon and kaon is misidentified as muon and peaking for $B^+ \to K^+\mu^+\mu^-$ channel. We have assigned the faking particle mass while calculating the veto window, which is $M_{K^+\mu^-} \notin (3.06-3.13)$ GeV/c^2. The small contribution from charmless B decays, $B \to K\pi^+\pi^-$, for modes with muon final states are kept fixed in the fit.

We determine the signal yield by performing extended maximum likelihood fit in three dimentions namely M_{bc}, ΔE and $\mathscr{O}'$. The signal probability density function (PDF) is calibrated using $B \to J/\psi(\to \ell^+\ell^-)K$ sample. The continuum background is calibrated using off-resonance data sample. This off-resonance yields are scaled according to luminosity and cross-section and are fixed in the fit. The results of the fit projected in a signal-enhanced region [$M_{\rm bc} \in (5.27, 5.29)\,{\rm GeV}/c^2$, $|\Delta E| < 0.05\,{\rm GeV}$ and $\mathscr{O}' \in (1.0, 8.0)$] for $M_{\rm bc}$, ΔE and $\mathscr{O}'$ distributions in the data sample are demonstrated for $B^+ \to K^+\mu^+\mu^-$ and $B^+ \to K^+e^+e^-$ channels in Figs. 3. The fit is also per-

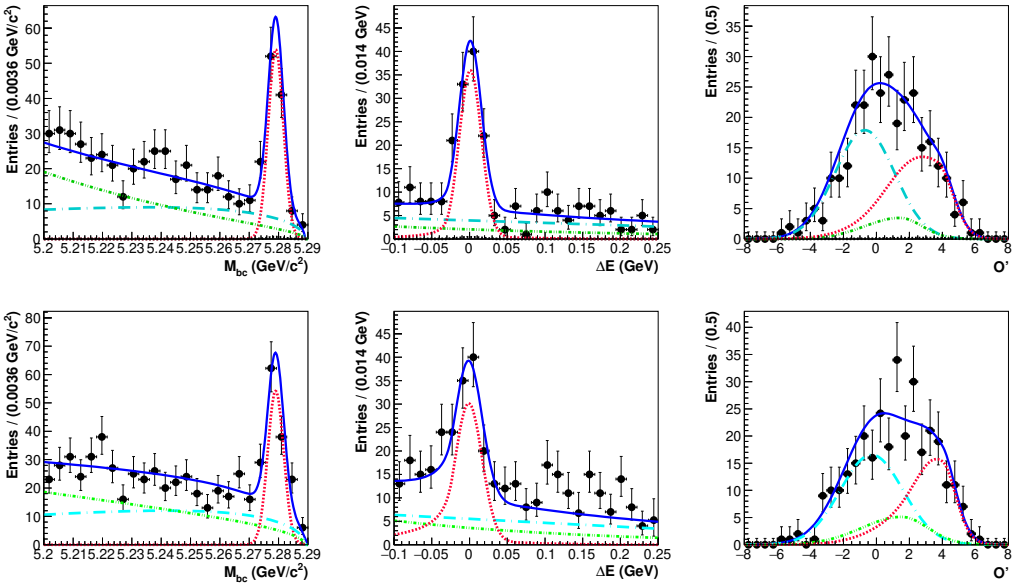

Figure 3: Signal enhanced $M_{\rm bc}$(left), ΔE (middle), and $\mathscr{O}'$ (right) projections of three-dimensional unbinned extended maximum-likelihood fits to the data events that pass the selection criteria for $B^+ \to K^+\mu^+\mu^-$ (top), and $B^+ \to K^+e^+e^-$ (bottom). Points with error bars are the data; blue solid curves are the fitted results for the signal-plus-background hypothesis; red dashed curves denote the signal component; cyan big dashed, green dashed-dotted, and black dashed curves represent continuum, $B\bar{B}$ background, and $B \to$ charmless decays, respectively.

formed in $B^0 \to K^0_S\ell^+\ell^-$ mode, and in the abovementioned four q^2 bins including the bin $1 < q^2 < 6$ GeV$^2/c^4$, where LHCb result shows deviation. From these fit results, R_K and A_I are calculated using Eqs. (1.1) and (1.2), respectively. The results of R_{K^+} and R_{K^0} for different q^2 bins are found to be consistent with SM expectation. The R_K, which is the weighted average of R_{K^+} and R_{K^0}, is also consistent with SM prediction and are shown in Fig. 4. The A_I has negative asymmetry for almost all the bins. The highest deviation is found for $q^2 \in (1.0, 6.0)$ bin for mode with muon

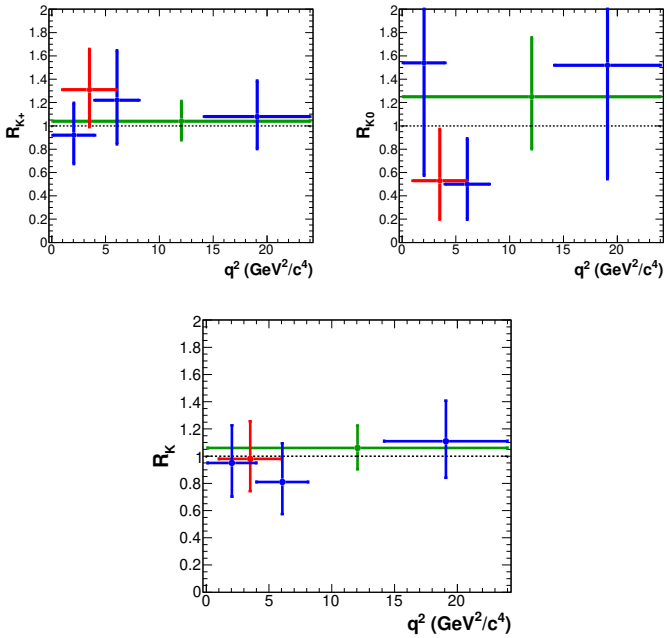

Figure 4: R_K in bins of q^2, for $B^+ \to K^+\ell^+\ell^-$ (upper left), $B^0 \to K^0_S\ell^+\ell^-$ (upper right), and combining both modes (lower). The red marker represents the bin of $1 < q^2 < 6$ GeV$^2/c^4$, and the blue markers are for $0.1 < q^2 < 4$, $4 < q^2 < 8.12$ and $q^2 > 14.18$ GeV$^2/c^4$ bins. The green marker denotes the whole q^2 region excluding the charmonium resonances.

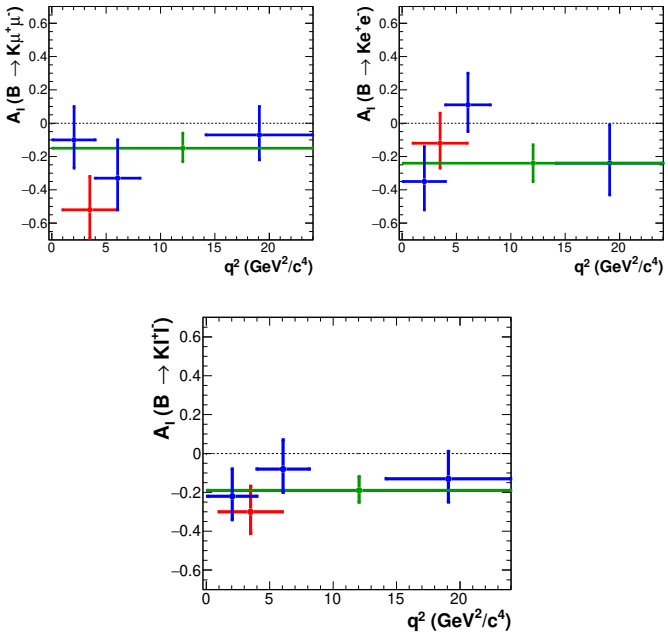

Figure 5: A_I measurements in bins of q^2, for decays $B \to K\mu^+\mu^-$ (upper left), $B \to Ke^+e^-$ (upper right), and combining both modes (lower). The legends are the same as in Fig. 4.

final states and has a deviation of 2.7σ. The A_I plots $B \to K\mu^+\mu^-$, $B \to Ke^+e^-$ and both modes combined are shown in Fig. 5.

5. Conclusion

In summary, we have measured the lepton flavor universality ratios, R_{K^*} and R_K for the decays $B \to K^*\ell^+\ell^-$ and $B \to K\ell^+\ell^-$ as a function of q^2. The values for different q^2 bins are consistent with the SM prediction. Our result for the bin of interest, $q^2 \in (1.0, 6.0)\,\mathrm{GeV}^2/c^4$, is consistent with LHCb [5, 16] result, which has a deviation of 2.5σ, as well as the SM expectation. The isospin asymmetry, A_I, of $B \to K\ell^+\ell^-$ mode for almost all the bins for different channels have negative asymmetry. For the bin $q^2 \in (1.0, 6.0)\,\mathrm{GeV}^2/c^4$, the obtained A_I value deviates from zero by 2.7σ for the mode with muon final states.

6. Acknowledgments

We thank the KEKB group for excellent operation of the accelerator; the KEK cryogenics group for efficient solenoid operations; and the KEK computer group, the NII, and PNNL/EMSL for valuable computing and SINET5 network support. We acknowledge support from MEXT, JSPS and Nagoya's TLPRC (Japan); ARC (Australia); FWF (Austria); NSFC and CCEPP (China); MSMT (Czechia); CZF, DFG, EXC153, and VS (Germany); DST (India); INFN (Italy); MOE, MSIP, NRF, RSRI, FLRFAS project and GSDC of KISTI and KREONET/GLORIAD (Korea); MNiSW and NCN (Poland); MSHE (Russia); ARRS (Slovenia); IKERBASQUE (Spain); SNSF (Switzerland); MOE and MOST (Taiwan); and DOE and NSF (USA).

References

[1] G. Hiller and F. Kruger, Phys. Rev. D **69**, 074020 (2004).

[2] C. Bobeth, G. Hiller, and G. Piranishvili, JHEP **12** (2007) 040.

[3] M. Bauer and M. Neubert, Phys. Rev. Lett. **116**, 141802 (2016).

[4] R. Aaij *et al.* (LHCb Collaboration), JHEP **08** (2017) 055.

[5] R. Aaij *et al.* (LHCb Collaboration), Phys. Rev. Lett. **122**, 191801 (2019).

[6] J. T. Wei *et al.* (Belle Collaboration), Phys. Rev. Lett. **103**, 171801 (2009).

[7] T. Feldmann and J. Matias, JHEP **0301** (2003) 074.

[8] M. Tanabashi *et al.* (Particle Data Group), Phys. Rev. D **98**, 030001.

[9] J. Lyon and R. Zwicky, Phys. Rev. D **88**, 094004 (2013).

[10] J. P. Lees *et al.* (BaBar Collaboration), Phys. Rev. D **86**, 032012 (2012).

[11] R. Aaij *et al.* (LHCb Collaboration), JHEP **06** (2014) 133.

[12] A. Abashian *et al.* (Belle Collaboration), Nucl. Instrum. Methods Phys. Res., Sec. A **479**, 117 (2002); also, see the detector section in J. Brodzicka *et al.* , Prog. Theor. Exp. Phys. **2012**, 04D001 (2012).

[13] Z. Natkaniec *et al.* (Belle SVD2 Group), Nucl. Instrum. Methods Phys. Res., Sec. A **560**, 1 (2006).

[14] A. Abdesselam *et al.* (Belle Collaboration), arXiv:1904.02440

[15] A. Abdesselam *et al.* (Belle Collaboration), arXiv:1908.01848

[16] R. Aaij *et al.* (LHCb Collaboration), Phys. Rev. Lett. **113**, 151601 (2014).